Efficient solution processed bulk-heterojunction solar cells based a donor–acceptor oligothiophene†

Yongsheng Liu,[a] Xiangjian Wan,*[a] Bin Yin,[b] Jiaoyan Zhou,[a] Guankui Long,[a] Shougen Yin[b] and Yongsheng Chen*[a]

Received 30th November 2009, Accepted 8th January 2010
First published as an Advance Article on the web 8th February 2010
DOI: 10.1039/b925048d

A solution processed small molecule with low band gap, dicyanovinyl-substituted oligothiophene (DCN7T), was used as the donor in bulk heterojunctions solar cells and a power conversion efficiency of 2.45% has been obtained for the device using simply spin-coating without special treatment.

Introduction

Organic solar cells using conjugated molecular materials has become increasingly feasible through the development of bulk heterojunction (BHJ) structures based on intimate blends of polymeric donors and soluble fullerene acceptors,[1–4] where efficient exciton separation is enabled by a large-area donor–acceptor interface.[5,6] The attractive features of this type of solar cell include the ease of solution-processing, low costs, light weight, and the potential application in flexible large-area devices.[7,8] So far, such devices based on polymer/fullerene blends have achieved high power conversion efficiencies (PCEs) of more than 6%.[9–12]

In recent years, bulk heterojunctions (BHJ) solar cells utilizing solution-processable small molecules as the active layer have been also actively studied.[13–22] Although the power conversion efficiencies (PCEs) are still behind those of polymer-based devices, solution-processable small molecule-based solar cells have the advantage that, for example, they are easier to synthesize and purify, are intrinsically monodisperse, have well-tunable physicochemical properties, provide important reproducibility in device fabrication, and typically show higher charge carrier mobilities.[23] At the same time, devices of this class can improve the efficiency of the process and greatly reduce fabrication costs, compared with the vacuum-deposited small molecule-based devices. Up to now, the best results of organic photovoltaic cells made by solution-processable small molecules heterostructures were reported by Nguyen[20–22] and coworkers, the PCEs have been improved to 2.3%, 3.0% and 4.4% very recently.

Oligothiophenes with well defined structures possess extensive π-electron delocalization along the molecular backbone and are well known as high hole-transporting materials. Acceptor-substituted oligothiophenes with a highly polarizable π-electron systems have been widely investigated for their photovoltaic properties.[15,20–22,24–26] This class of materials can extend the absorption spectrum of the donor toward longer wavelengths by an intramolecular charge transfer and thus have a good match with the solar spectrum.[15] The dicyanovinyl group has strong electron-accepting properties and its double bond can also participate in the conjugation of the whole backbone π-system and lead to efficient intramolecular charge transfer. Some dicyanomethylene-substituted oligothiophenes have been synthesized and used for solar cells,[15,24–26] but solution-processable oligothiophenes of this class as photoactive layer for use in solar cells are rarely studied.

Recently, we reported the synthesis of an acceptor–donor–acceptor molecule DCN7T (Fig. 1) with a narrow optical band gap.[27] Moreover, the optical spectra of their films show a very good solar spectral coverage. These properties, coupled with their good solubility and stability, prompt us to study their applications in solar cells. In this paper, we report the use of this new solution processable acceptor-substituted oligothiophene as a donor and [6,6]-phenyl-C_{61}-butyric acid methyl ester (PCBM) (Fig. 1) as a acceptor in BHJ solar cells, which show a PCE of 2.45%. Our results suggest that DCN7T is promising for developing efficient solution-processed BHJ solar cells based on small molecules.

Experimental

Synthesis and instruments

The dicyanovinyl-substituted oligothiophene, DCN7T (Fig. 1), was synthesized following our previously reported procedure.[27]

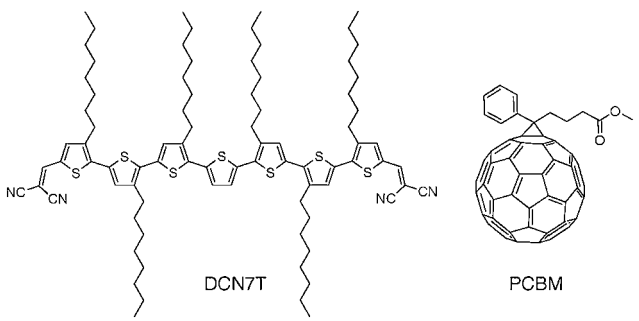

Fig. 1 Chemical structure of DCN7T and PCBM.

[a]*Key Laboratory for Functional Polymer Materials and Centre for Nanoscale Science and Technology, Institute of Polymer Chemistry, College of Chemistry, Nankai University, Tianjin, 300071, China. E-mail: xjwan@nankai.edu.cn; yschen99@nankai.edu.cn; Fax: +86-22-23499992; Tel: +86-22-23500693*
[b]*Key Laboratory of Display Materials and Photoelectric Devices, Ministry of Education, Institute of Material Physics, Tianjin University of Technology, Tianjin, 300384, People's Republic of China*
† Electronic supplementary information (ESI) available: Complete device fabrication methods; fluorescence emission spectra; detailed information on film AFM images. See DOI: 10.1039/b925048d

UV–vis spectra were obtained with a JASCO V-570 spectrophotometer. Fluorescence spectra (ESI†) were obtained with a FluoroMax-P instrument. X-Ray diffraction (XRD) experiments were performed on a Rigaku D/max-2500 X-ray powder diffractometer with Cu-Kα radiation ($k = 1.5406$ Å) at a generator voltage of 40 kV and a current of 100 mA. AFM studies were performed using a Digital Instruments Dimension 3100 microscope in the tapping mode.

Charaterization and photovoltaic devices

Hole mobility was measured according to a method based on the space charge limited current (SCLC) model.[11,28,29] BHJ solar cells were fabricated by use of a common process with the structure of ITO/PEDOT:PSS/DCN7T:PCBM/LiF/Al. Current–voltage (*J–V*) characteristics of the photovoltaic devices were measured in air using a Keithley SMU 2400 unit. Details about the experimental procedures and equipment can be found in the ESI.†

Results and discussion

Optical absorption

Fig. 2 shows the film (from $CHCl_3$) absorption spectra of DCN7T and DCN7T/PCBM with different blend ratios (1 : 1, 1 : 1.4, 1 : 1.8, w/w) of weight-to-weight. The film absorption of DCN7T extends up to 800 nm and shows a shoulder peak structure at even longer wavelength, which suggests a vibronic progression enforced by strong intermolecular interactions.[24,30] It can be seen that, although PCBM exhibits weak absorption in the visible range, the absorption band of DCN7T below 600 nm were largely increased after PCBM was added. The blended film gives a very good solar spectral coverage. As the amount of PCBM increases, the peak at 337 nm assigned to PCBM increases in intensity. However, for the absorption band between 400 to 600 nm, the intensity of the absorption band decreases when the DCN7T/PCBM blend ratio increased to 1 : 1.8 (w/w), as previously observed for conjugated polymers where more PCBM inhibits crystallization.[21,31] Because of the same reason, a slight blue-shift of 4 nm of DCN7T band was observed when the blend ratio was 1 : 1.8 (w/w).

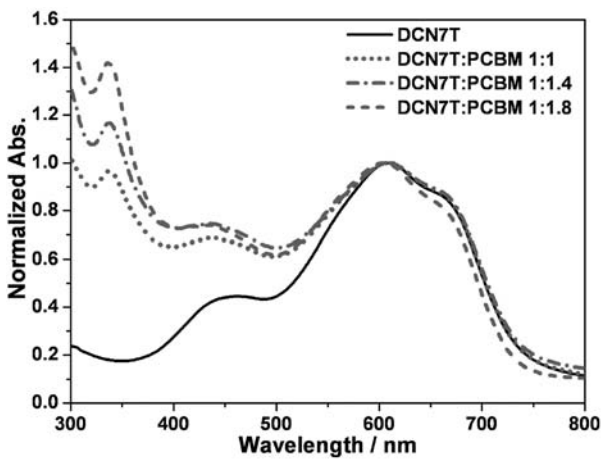

Fig. 2 Normalized absorption spectra of blend films spin-cast from chloroform solutions of DCN7T and DCN7T/PCBM with different ratios (w/w).

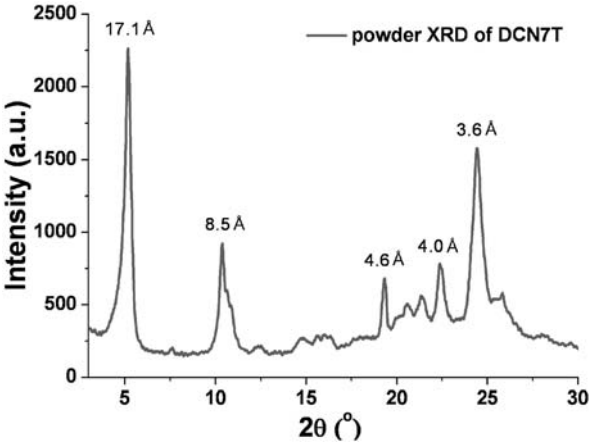

Fig. 3 X-Ray diffraction patterns of DCN7T powder. Peaks are labeled with *d*-spacing in angstroms. The sharp diffraction peaks indicate that the oligomer formed an ordered structure in the solid state.

X-Ray diffraction (XRD)

To investigate the crystallinity of dicyanomethylene-substituted oligothiophene in the solid state, an XRD pattern was collected on a powder sample of DCN7T (Fig. 3). The first strong and sharp diffraction peak at 5.2° indicates a well-organized molecular structure, which reveals that the distance between DCN7T main chains separated by alkyl side chains is 17.1 Å.[32] The diffraction peak at 2θ of 10.4°, corresponding to a *d*-spacing of 8.5 Å, was attributed to some correlations of alkyl chains between neighboring molecules. Then, the peak at 19.3° and 22.4°, which corresponding to a *d*-spacing of 4.6 and 4.0 Å, are the short-range correlations of the alkyl chains. The sharp peak at 24.5° reveals a short π–π distance of 3.6 Å between the oligothiophene backbone, indicating the DCN7T main chain is of planar conformation in the solid state, and this lattice distance is very close to that observed in P3OT (3.8 Å).[33]

Charge transport of DCN7T

The hole mobility of the pristine DCN7T is measured to be ~1.5 $\times$ 10^{-4} cm^2 V^{-1} s^{-1} according to method based on the space charge limited current (SCLC) model,[11,28,29] and the result is plotted in Fig. 4. This value is higher than hole mobilities measured for small molecules (*i.e.*, ~10^{-6} cm^2 V^{-1} s^{-1} for triphenylamine derivatives,[34] and ~10^{-6}–10^{-5} cm^2 V^{-1} s^{-1} for oligothiophene and diketopyrrolopyrrole derivatives,[21,22] as determined by using the SCLC model) that are used as electron donors for solar cells. The hole mobility of DCN7T is comparable to that of the widely used donor polymer poly(3-hexylthiophene) (P3HT), which have a typical value of (1.4–3.0) $\times$ 10^{-4} cm^2 V^{-1} s^{-1}.[29] The π-electron delocalization, planarity of the oligothiophene backbone and the π–π stacking observed from the XRD data above are believed to be directly responsible for the high SCLC mobility of DCN7T. Thus, DCN7T is expected to be a promising candidate for solar cell applications as an electron donor material.

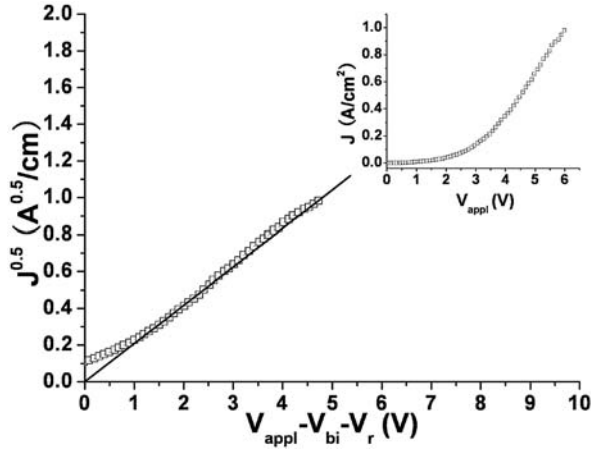

Fig. 4 $J^{0.5}$ *vs.* V plots for the DCN7T film at room temperature. The solid lines are fits of the data points. The inset depicts the J *vs.* V_{appl} plot of the devices from the DCN7T before correction for the applied voltage.

Energy levels

The HOMO and LUMO levels (Fig. 5b) of DCN7T was measured by electrochemical cyclic voltammetry (CV).[22] The electrochemical band gap is 1.71 eV, consistent with the optical band gap (1.68 eV).[27] The low band gap, relevant energy level positions (Fig. 5b), high SCLC mobility, good solar spectrum match and solubility indicate that DCN7T should be an effective donor in BHJ devices.

Photovoltaic properties

BHJ solar cells with structure (Fig. 5a) of ITO/PEDOT:PSS/DCN7T:PCBM/LiF/Al using DCN7T as electron donor and PCBM as electron acceptor were fabricated. After spin-coating a hole extraction/electron-blocking layer, a 40 nm layer of PEDOT:PSS, onto a pre-cleaned indium-tin oxide (ITO) coated glass substrate, the DCN7T(8 mg mL^{-1})/PCBM (1 : 1, 1 : 1.4, 1 : 1.8, w/w) blends in $CHCl_3$ was spincoated in air. The thickness of the photoactive layer of all devices was approximately 110 nm. After drying, the cells were then completed by sequential thermal vacuum deposition of LiF (1 nm) and Al (70 nm) as the cathode with an area of ~9 mm^2.

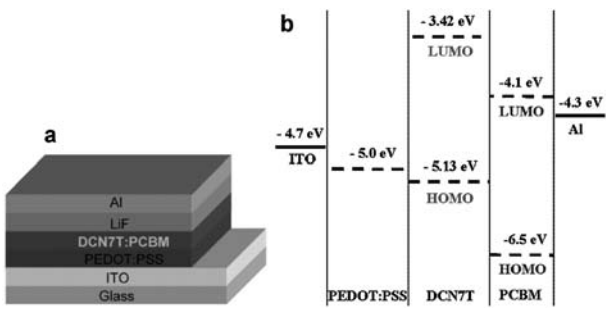

Fig. 5 (a) Schematic of the device with DCN7T/PCBM thin film as the active layer and the structure ITO/PEDOT:PSS (40 nm)/DCN7T:PCBM (110 nm)/LiF (1 nm)/Al (70 nm). (b) Band diagram for the DCN7T/PCBM based device.

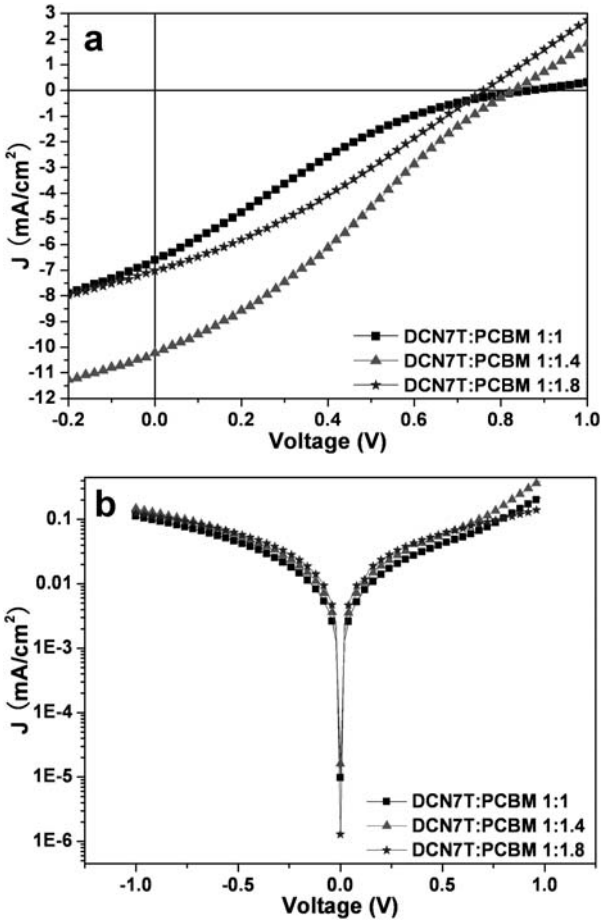

Fig. 6 BHJ devices based on DCN7T/PCBM with different blend ratios (w/w): (a) J–V characteristics under AM 1.5G irradiation (100 mW cm^{-2}); (b) logarithmic J–V characteristics in the dark.

Fig. 6 shows the current density *versus* voltage (J–V) curves for devices using a varied blend ratios (1 : 1, 1 : 1.4, 1 : 1.8, w/w) of DCN7T (8 mg mL^{-1}) and PCBM under AM 1.5G simulated solar illumination at an intensity of 100 mW cm^{-2}. Increasing the concentration of PCBM in the blend has a strong impact on the short circuit current density (J_{sc}), while the open circuit voltage (V_{oc}) is much less dependent on the concentration of PCBM (Table 1) as it is related to the nature of the components and less to the morphology.[35,36] The devices for a 1 : 1 blend ratio exhibits a J_{sc} of 6.61 mA cm^{-2}, a V_{oc} of 0.88 V and a fill factor (FF) of 18.9%, which yields a PCE (η) of 1.10%. But with increasing the donor–acceptor blend ratios from 1 : 1 to 1 : 1.8, the J_{sc} first increased and then decreased, but the FF increased to 31.5%. The best PCE was obtained when the ratio is 1 : 1.4, which gave a J_{sc} of 10.23 mA cm^{-2}, a V_{oc} of 0.82 V, and thus a PCE of 2.45% was

Table 1 Effect of DCN7T/PCBM blend ratio on the device characteristics

Active layer (w/w)	J_{sc}/mA cm^{-2}	V_{oc}/V	FF (%)	η (%)
DCN7T/PCBM (1 : 1)	6.61	0.88	18.9	1.10
DCN7T/PCBM (1 : 1.4)	10.23	0.82	29.2	2.45
DCN7T/PCBM (1 : 1.8)	7.03	0.74	31.5	1.64

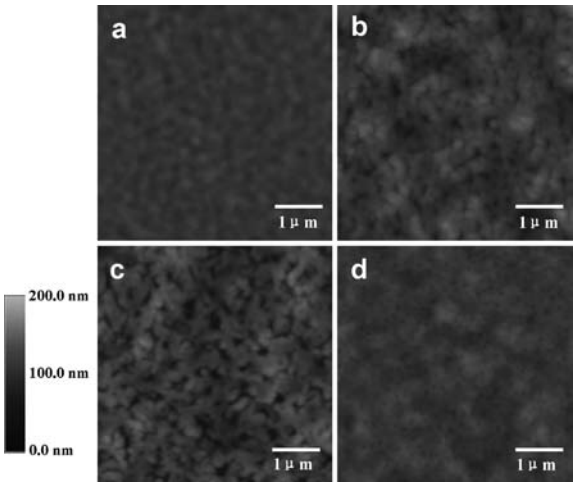

Fig. 7 AFM topography images (5 μm × 5 μm) of films cast from chloroform solutions of the blend of DCN7T/PCBM with the following ratios (w/w): (a) 1 : 0, (b) 1 : 1, (c) 1 : 1.4, and (d) 1 : 1.8. Note that the contrast scale for all the films is 0–200 nm.

achieved with a FF of 29.2%. The decrease of J_{sc} to 7.03 mA cm^{-2} for the ratio of 1 : 1.4 to 1 : 1.8 is believed to due to the fact that the saturating in the active layer with PCBM leads to phase separation as reported in the literature.[37] Combined with a V_{oc} of 0.74 V and a FF of 31.5%, the device using the 1 : 1.8 ratio yields a PCE of 1.64%. Interestingly, we found that the device performance is generally lower when other solvents, such as dichlorobenzene or chlorobenzene, were used to replace chloroform. It should be noted that the *J*–*V* curves, as shown in Fig. 6a for the donor–acceptor blend ratios of 1 : 1 and 1 : 1.4, show an inflection point (kink), which were reported previously and were attributed to a carrier transport problem.[38–41]

Morphology

Fig. 7 shows the surface topography, measured by AFM, of the films cast from chloroform solutions of the blend of DCN7T/PCBM with different ratios. Pure DCN7T film was included in the study for comparison. Some ordered aggregation because of π–π stacking was observed for the film of DCN7T and its root-mean-square (rms) roughness was 4.96 nm. After PCBM was added, all the films show visible phase separation with an elongated and ordered network of donor/acceptor domains. The surface of the DCN7T/PCBM film with a blend ratio of 1 : 1.4 is significantly rougher (rms roughness is 14.26 nm) than those with a blend ratio of 1 : 1 (rms roughness is 11.13 nm) and 1 : 1.8 (rms roughness is 6.61 nm). The rough surface may increase the heterojunction area and effectively reduce the charge-transport distance and at the same time provide a nano-scaled texture that further enhances internal light absorption.[42,43] This continuous and rough film morphology combined with the good solar spectral coverage of the film can account for the high photovoltaic performance for the donor/acceptor blend ratio of 1 : 1.4 (w/w).

Conclusions

In conclusion, with small molecule of dicyanovinyl-substituted oligothiophene as the electron donor, we have fabricated BHJ solar cells and a PCE of 2.45% has been obtained for the devices simply using spin-coating without special treatment. This result indicates that higher power conversion efficiency, comparable to or even better than that of solution-processed polymer-based BHJ devices, should be achievable for small molecules, which have the advantages for monodisperse structure and repeatable performance.

Acknowledgements

The authors gratefully acknowledge the financial support from the NSFC (#20774047), MOST (#2006CB932702), MOE (#708020) of China and NSF of Tianjin City (#07JCYBJC03000 and #08JCZDJC25300).

Notes and references

1 A. Dhanabalan, J. K. J. van Duren, P. A. van Hal, J. L. J. van Dongen and R. A. J. Janssen, *Adv. Funct. Mater.*, 2001, **11**, 255.
2 P. Peumans, S. Uchida and S. R. Forrest, *Nature*, 2003, **425**, 158.
3 P. Schilinsky, U. Asawapirom, U. Scherf, M. Biele and C. J. Brabec, *Chem. Mater.*, 2005, **17**, 2175.
4 M. M. Wienk, J. M. Kroon, W. J. H. Verhees, J. Knol, J. C. Hummelen, P. A. van Hal and R. A. J. Janssen, *Angew. Chem., Int. Ed.*, 2003, **42**, 3371.
5 N. S. Sariciftci, L. Smilowitz, A. J. Heeger and F. Wudl, *Science*, 1992, **258**, 1474.
6 J. J. M. Halls, C. A. Walsh, N. C. Greenham, E. A. Marseglia, R. H. Friend, S. C. Moratti and A. B. Holmes, *Nature*, 1995, **376**, 498.
7 G. Yu, J. Gao, J. C. Hummelen, F. Wudl and A. J. Heeger, *Science*, 1995, **270**, 1789.
8 J. Y. Kim, K. Lee, N. E. Coates, D. Moses, T. Q. Nguyen, M. Dante and A. J. Heeger, *Science*, 2007, **317**, 222.
9 H. Y. Chen, J. H. Hou, S. Q. Zhang, Y. Y. Liang, G. W. Yang, Y. Yang, L. P. Yu, Y. Wu and G. Li, *Nat. Photonics*, 2009, **3**, 649.
10 S. H. Park, A. Roy, S. Beaupré, S. Cho, N. Coates, J. S. Moon, D. Moses, M. Leclerc, K. Lee and A. J. Heeger, *Nat. Photonics*, 2009, **3**, 297.
11 Y. Y. Liang, D. Q. Feng, Y. Wu, S. T. Tsai, G. Li, C. Ray and L. P. Yu, *J. Am. Chem. Soc.*, 2009, **131**, 7792.
12 J. H. Hou, H. Y. Chen, S. Q. Zhang, R. I. Chen, Y. Yang, Y. Wu and G. Li, *J. Am. Chem. Soc.*, 2009, **131**, 15586.
13 O. Hagemann, M. Jorgensen and F. C. Krebs, *J. Org. Chem.*, 2006, **71**, 5546.
14 L. Schmidt-Mende, A. Fechtenkotter, K. Mullen, E. Moons, R. H. Friend and J. D. MacKenzie, *Science*, 2001, **293**, 1119.
15 S. Roquet, A. Cravino, P. Leriche, O. Aleveque, P. Frere and J. Roncali, *J. Am. Chem. Soc.*, 2006, **128**, 3459.
16 F. Silvestri, M. D. Irwin, L. Beverina, A. Facchetti, G. A. Pagani and T. J. Marks, *J. Am. Chem. Soc.*, 2008, **130**, 17640.
17 C. Q. Ma, M. Fonrodona, M. C. Schikora, M. M. Wienk, R. A. J. Janssen and P. Bauerle, *Adv. Funct. Mater.*, 2008, **18**, 3323.
18 M. T. Lloyd, A. C. Mayer, S. Subramanian, D. A. Mourey, D. J. Herman, A. V. Bapat, J. E. Anthony and G. G. Malliaras, *J. Am. Chem. Soc.*, 2007, **129**, 9144.
19 C. H. Huang, N. D. McClenaghan, A. Kuhn, J. W. Hofstraat and D. M. Bassani, *Org. Lett.*, 2005, **7**, 3409.
20 A. B. Tamayo, X. D. Dang, B. Walker, J. Seo, T. Kent and T. Q. Nguyen, *Appl. Phys. Lett.*, 2009, **94**, 103301.
21 A. B. Tamayo, B. Walker and T. Q. Nguyen, *J. Phys. Chem. C*, 2008, **112**, 11545.
22 B. Walker, A. B. Tamayo, X. D. Dang, P. Zalar, J. H. Seo, A. Garcia, M. Tantiwiwat and T. Q. Nguyen, *Adv. Funct. Mater.*, 2009, **19**, 3063.
23 I. N. Hulea, S. Fratini, H. Xie, C. L. Mulder, N. N. Iossad, G. Rastelli, S. Ciuchi and A. F. Morpurgo, *Nat. Mater.*, 2006, **5**, 982.
24 C. Uhrich, R. Schueppel, A. Petrich, M. Pfeiffer, K. Leo, E. Brier, P. Kilickiran and P. Baeuerle, *Adv. Funct. Mater.*, 2007, **17**, 2991.
25 K. Schulze, C. Uhrich, R. Schuppel, K. Leo, M. Pfeiffer, E. Brier, E. Reinold and P. Bauerle, *Adv. Mater.*, 2006, **18**, 2872.
26 P. F. Xia, X. J. Feng, J. P. Lu, S. W. Tsang, R. Movileanu, Y. Tao and M. S. Wong, *Adv. Mater.*, 2008, **20**, 4810.

27 Y. S. Liu, J. Y. Zhou, X. J. Wan and Y. S. Chen, *Tetrahedron*, 2009, **65**, 5209.
28 P. W. M. Blom, M. J. M. de Jong and M. G. van Munster, *Phys. Rev. B: Condens. Matter*, 1997, **55**, R656.
29 V. D. Mihailetchi, H. X. Xie, B. de Boer, L. J. A. Koster and P. W. M. Blom, *Adv. Funct. Mater.*, 2006, **16**, 699.
30 M. Turbiez, P. Frere, M. Allain, C. Videlot, J. Ackermann and J. Roncali, *Chem.–Eur. J.*, 2005, **11**, 3742.
31 C. Melzer, E. J. Koop, V. D. Mihailetchi and P. W. M. Blom, *Adv. Funct. Mater.*, 2004, **14**, 865.
32 B. C. Thompson, B. J. Kim, D. F. Kavulak, K. Sivula, C. Mauldin and J. M. J. Fréchet, *Macromolecules*, 2007, **40**, 7425.
33 S. Samitsu, T. Shimomura, S. Heike, T. Hashizume and K. Ito, *Macromolecules*, 2008, **41**, 8000.
34 C. He, Q. G. He, X. D. Yang, G. L. Wu, C. H. Yang, F. L. Bai, Z. G. Shuai, L. X. Wang and Y. F. Li, *J. Phys. Chem. C*, 2007, **111**, 8661.
35 M. C. Scharber, D. Wuhlbacher, M. Koppe, P. Denk, C. Waldauf, A. J. Heeger and C. L. Brabec, *Adv. Mater.*, 2006, **18**, 789.
36 A. Gadisa, M. Svensson, M. R. Andersson and O. Inganas, *Appl. Phys. Lett.*, 2004, **84**, 1609.
37 J. K. J. van Duren, X. N. Yang, J. Loos, C. W. T. Bulle-Lieuwma, A. B. Sieval, J. C. Hummelen and R. A. J. Janssen, *Adv. Funct. Mater.*, 2004, **14**, 425.
38 F. C. Krebs and K. Norrman, *Progr. Photovolt.: Res. Appl.*, 2007, **15**, 697.
39 M. Glatthaar, M. Riede, N. Keegan, K. Sylvester-Hvid, B. Zimmermann, M. Niggemann, A. Hinsch and A. Gombert, *Sol. Energy Mater. Sol. Cells*, 2007, **91**, 390.
40 M. Vogel, S. Doka, Ch. Breyer, M. Ch. Lux-Steiner and K. Fostiropoulos, *Appl. Phys. Lett.*, 2006, **89**, 163501.
41 S. T. Zhang, Y. C. Zhou, J. M. Zhao, Y. Q. Zhan, Z. J. Wang, Y. Wu, X. M. Ding and X. Y. Hou, *Appl. Phys. Lett.*, 2006, **89**, 043502.
42 Y. T. Chang, S. L. Hsu, G. Y. Chen, M. H. Su, T. A. Singh, E. W. G. Diau and K. H. Wei, *Adv. Funct. Mater.*, 2008, **18**, 2356.
43 G. Li, V. Shrotriya, J. S. Huang, Y. Yao, T. Moriarty, K. Emery and Y. Yang, *Nat. Mater.*, 2005, **4**, 864.

Supplementary Material (ESI) for *Journal of Materials Chemistry*

Supplementary data

Efficient Solution Processed Bulk-Heterojunction Solar Cells Based a Donor-Acceptor Oligothiophene

Yongsheng Liu,[a] Xiangjian Wan,*[a] Bin Yin,[b] Jiaoyan Zhou,[a] Guankui Long,[a] Shougen Yin,[b] Yongsheng Chen*[a]

[a] *Key Laboratory for Functional Polymer Materials and Centre for Nanoscale Science and Technology, Institute of Polymer Chemistry, College of Chemistry, Nankai University, Tianjin 300071, China.* [b] *Key Laboratory of Display Materials and Photoelectric Devices, Ministry of Education, Institute of Material Physics, Tianjin University of Technology, Tianjin 300384, People's Republic of China.*

E-mail: yschen99@nankai.edu.cn

Hole mobility measurement

Hole mobility was measured according to a similar method described in the literature, using a diode configuration of ITO/PEDOT:PSS/DCN7T/Al by taking current-voltage current in the range of 0-6 V and fitting the results to a space charge limited form, where the SCLC is described by

$$J = 9\varepsilon_0\varepsilon_r\mu_h V^2/8L^3$$

where J is the current density, L is the film thickness of active layer, μ_h is the hole mobility, ε_r is the relative dielectric constant of the transport medium, ε_0 is the permittivity of free space (8.85×10^{-12} F/m), V is the internal voltage in the device and $V = V_{appl} - V_r - V_{bi}$, where V_{appl} is the applied voltage to the device, V_r is the voltage drop due to contact resistance and series resistance across the electrodes, and V_{bi} is the built-in voltage due to the relative work function difference of the two electrodes. The V_{bi} can be determined from the transition between the Ohmic region and the SCLC region and was found to be about 1.2 V.

Device fabrication

The photovoltaic device was fabricated by use of a common process. The ITO-coated glass substrates were cleaned by ultrasonic treatment in detergent, deionized water, isopropyl alcohol, and acetone under ultrasonication for 20 minutes each and subsequently dried in oven for 12 hours. A thin layer of PEDOT:PSS (Baytron PH 500) was spin-coated (4000 rpm, ca. 40nm thick) onto ITO surface. After being baked at 120 ^{o}C for 20 min, the active layer was then spin-cast from a varied weight-to-weight (1:1, 1:1.4, 1:1.8, w/w) mixture of DCN7T (8 mg mL^{-1}) and PCBM solution in chloroform at 500 rpm for 3 sec. and at 1300 rpm. for 9 sec on the ITO/PEDOT:PSS substrate without further special treatments. The active layer thickness was measured as ca. 110nm using a profilometer (Dektak 6M Stylus Profiler). After the film was transferred into a nitrogen filled glove box (< 0.1 ppm O^2 & H_2O), 1 nm LiF layer and 70nm Al layer were deposited in sequence on the active layer. The effective area of each cell is ~ 9 mm^2.

Current-Voltage measurement

All current–voltage (*J-V*) characteristics of the photovoltaic devices were measured in air using a Keithley SMU 2400 unit. A Xenon lamp with a filter (broadpasss GRB-3, Beijing Changtuo Scientific limited company) to simulate AM1.5G conditions was used as the excitation source with a power of 100 mW cm^{-2} white light illumination from the ITO side. Light source illumination intensity was measured using a calibrated broadband optical power meter (FZ-A, wave length range 400-1000 nm, Photoelectric Instrument Co, Beijing Normal University, China). The fabrication and measurement are conducted in air at room temperature. The calculation of the power conversion efficiency, η, has been performed using the following equation:

$$\eta = V_{oc} J_{sc} FF/P_{in}$$

where V_{oc}, J_{sc}, FF, and P_{in} are the open circuit voltage, the short circuit current density, the fill factor and the incident light power, respectively. The fill factor FF is determined according to $FF = (V_m J_m)/(V_{oc} J_{sc})$, where V_m and J_m are the voltage and the current density in the maximum power point of the *J–V* curve in the fourth quadrant.

Supplementary Figures

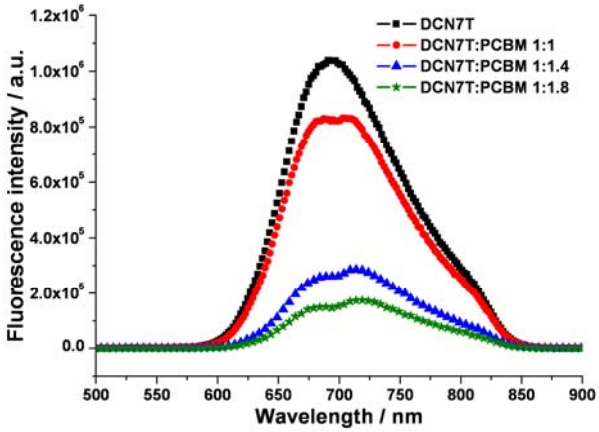

Fig. S1. Fluorescence emission spectra of DCN7T(0.16 mg ml^{-1})/PCBM with different blend ratios (w/w) in CHCl3 (λ_{ex} = 467 nm).

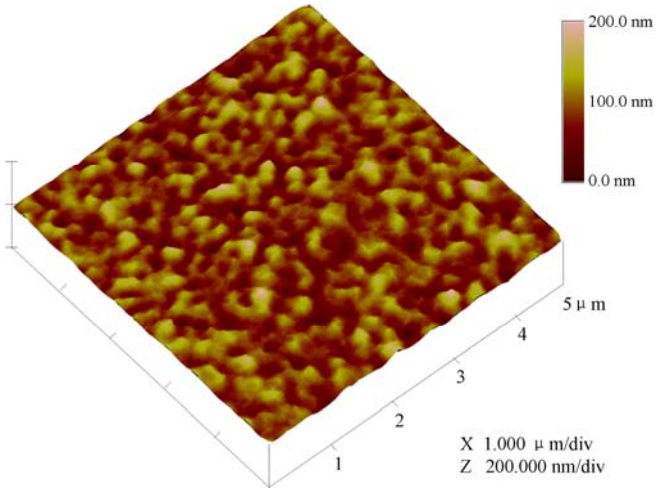

Fig. S2. AFM topography image(5µm × 5µm) of film cast from chloroform solution of DCN7T (3D image)

.

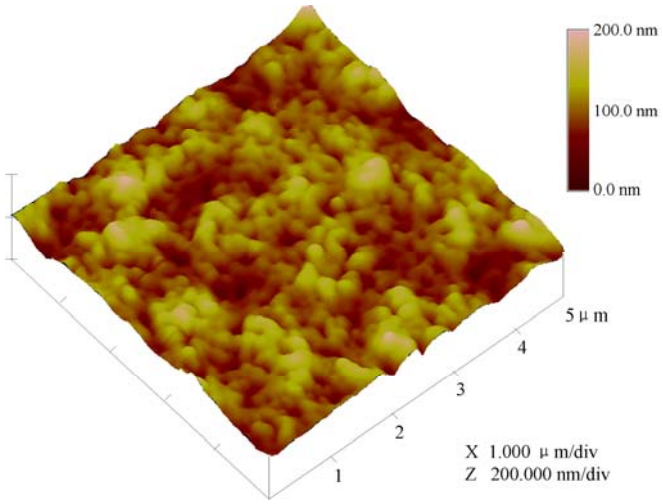

Fig. S3. AFM topography image (5 µm × 5 µm) of film cast from chloroform solution of the blend of DCN7T/PCBM with the ratio of 1:1 (w/w) (3D image).

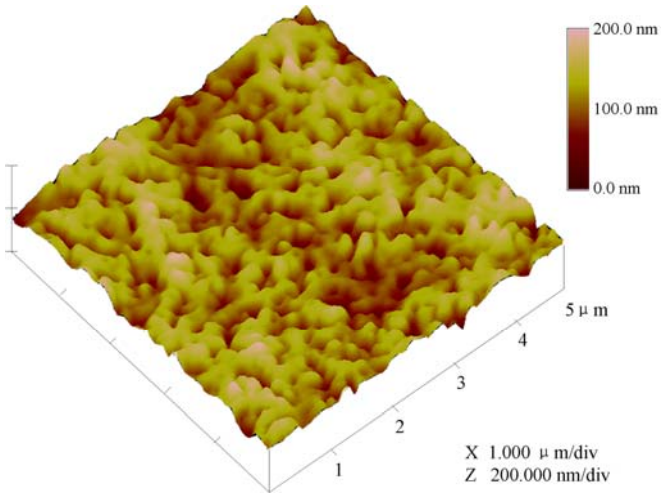

Fig. S4. AFM topography image (5 µm × 5 µm) of film cast from chloroform solution of the blend of DCN7T/PCBM with the ratio of 1:1.4 (w/w) (3D image).

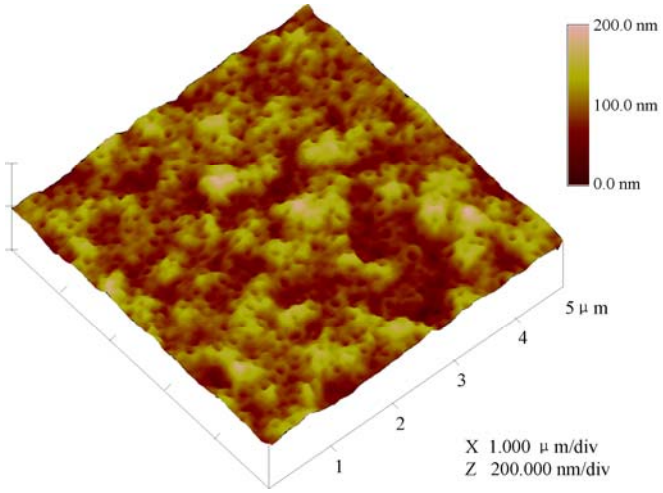

Fig. S5. AFM topography image (5 μm × 5 μm) of film cast from chloroform solution of the blend of DCN7T/PCBM with the ratio of 1:1.8 (w/w) (3D image).

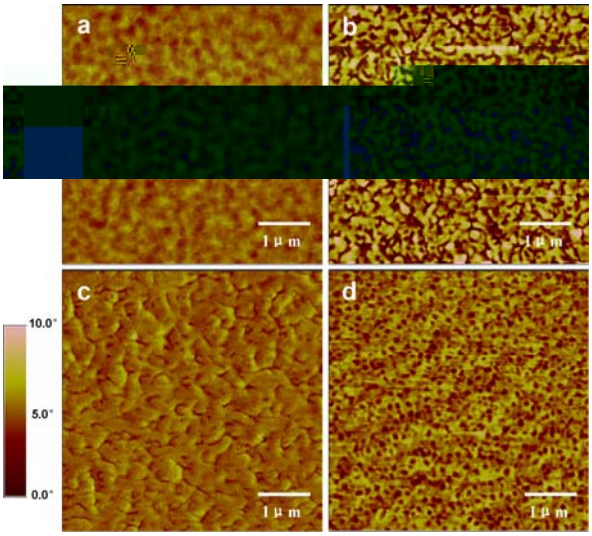

Fig. S6. AFM phase images (5 μm × 5 μm) of films cast from chloroform solutions of the blend of DCN7T/PCBM with the following ratios (w/w): (a) 1:0, (b) 1:1, (c) 1:1.4, and (d) 1:1.8.